

# Spurious resonances for substructured FEM-BEM coupling

Antonin Boisneault<sup>1,2</sup>, Marcella Bonazzoli<sup>2</sup>, Xavier Claeys<sup>1</sup>, and Pierre Marchand<sup>1</sup>

## 1 Introduction and definition of the problem

When solving the Helmholtz equation in complex heterogeneous media, it is of interest to decompose the domain according to the variation of the wavenumber. Local problems in homogeneous subdomains can be reformulated as equations set on their boundary (which is particularly useful for unbounded subdomains), and the global problem is solved with Finite Element Method - Boundary Element Method (FEM-BEM) coupling techniques [1, 5, 6]. Recently, a substructured formulation, called *Generalized Optimized Schwarz Method* (GOSM), has been designed for bounded domains, with weakly imposed boundary conditions, see [4], and extended in [2] to unbounded domains and interface conditions arising from several FEM-BEM coupling techniques. Unfortunately, FEM-BEM variational formulations can be ill-posed for certain wavenumbers called *spurious resonances* [11]. In this paper, we focus on the Johnson-Nédélec [6] and Costabel [5] couplings and show that the associated GOSMs suffer from that issue. For both couplings, we give an explicit expression of the kernel of the local operator associated with the interface between the FEM and BEM subdomains. This kernel and the one of the corresponding classical FEM-BEM couplings are simultaneously non-trivial.

For simplicity, we consider a three subdomains configuration. The impenetrable obstacle  $\Omega_O \subset \mathbb{R}^d$  ( $d = 2, 3$ ) is assumed connected Lipschitz bounded, with a connected complement  $\Omega := \mathbb{R}^d \setminus \overline{\Omega_O}$  decomposed into two connected Lipschitz subdomains:  $\Omega_F$  bounded with  $\partial\Omega_O \subseteq \partial\Omega_F$  and  $\Omega_B$  unbounded with bounded boundary, satisfying  $\Omega_F \cap \Omega_B = \emptyset$  (see Figure 1). We are interested in solving the following Helmholtz problem, which models time-harmonic acoustic wave propagation: find  $u \in H^1_{\text{loc}}(\Delta, \Omega)$  such that

---

<sup>1</sup> POEMS, CNRS, Inria, ENSTA, Institut Polytechnique de Paris, 91120 Palaiseau, France, e-mail: [antonin.boisneault@inria.fr](mailto:antonin.boisneault@inria.fr), [xavier.claeys@ensta.fr](mailto:xavier.claeys@ensta.fr), [pierre.marchand@inria.fr](mailto:pierre.marchand@inria.fr)

<sup>2</sup> Inria, Unité de Mathématiques Appliquées, ENSTA, Institut Polytechnique de Paris, 91120 Palaiseau, France, e-mail: [marcella.bonazzoli@inria.fr](mailto:marcella.bonazzoli@inria.fr)

$$\begin{cases} -\Delta u - \kappa^2 u = f, \text{ in } \Omega, \\ \text{boundary condition on } \partial\Omega, \\ \text{Sommerfeld's radiation condition,} \end{cases} \quad (1)$$

where the wavenumber  $\kappa: \Omega \rightarrow \mathbb{R}_{>0}$  is constant in  $\Omega_B$  and  $f \in L^2(\Omega_F)$ . See [10, Def. 2.6.1] for the definition of  $H_{\text{loc}}^1(\Delta, \Omega)$ , and [8, Sect. 2.2] for the Sommerfeld's radiation condition. Boundary conditions can be of Dirichlet, Neumann, Robin, or even mixed type, so  $\Omega_O$  can represent an impenetrable obstacle with a sound-soft or sound-hard boundary, for instance.

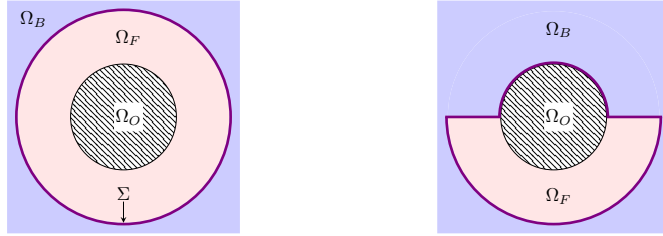


Fig. 1: Example of allowed (left) and forbidden (right) geometries (for simplicity).

In FEM-BEM coupling, the FEM is used for the (possibly) heterogeneous sub-domain  $\Omega_F$ , the BEM is applied for the homogeneous domain  $\Omega_B$ , and transmission conditions are imposed at the interface  $\Sigma := \partial\Omega_F \cap \partial\Omega_B$ . Our FEM-BEM formulation, based on the *Generalized Optimized Schwarz Method* (GOSM) [2, 4], is set on  $\Sigma$  and writes:

$$(\text{Id} + \Pi S)(q_B, q_F) = \mathbf{rhs}, \quad (2)$$

where  $\Pi$  is a (possibly) non-local exchange operator,  $S := \text{diag}(S_B, S_F)$  is a block-diagonal scattering operator and  $q_B, q_F \in H^{-1/2}(\Sigma)$  are outgoing impedance traces shared between  $\Omega_B$  and  $\Omega_F$ . More details about (2) can be found in [4, Propos. 8.1]. To derive the substructured formulation (2), the starting point is to write Problem (1) in variational form

$$\begin{aligned} \text{Find } u \in H^1(\Omega_F), p \in H^{-1/2}(\Sigma) \text{ such that } \forall v \in H^1(\Omega_F), \forall q \in H^{-1/2}(\Sigma) \\ \int_{\Omega_F} (\nabla u \cdot \nabla v - \kappa^2 uv) \, dx + \langle A_\Sigma(u|_\Sigma, p), (v|_\Sigma, q) \rangle = l_{\Omega_F}(v), \end{aligned} \quad (3)$$

where the explicit expression of  $A_\Sigma: H^{1/2}(\Sigma) \times H^{-1/2}(\Sigma) \rightarrow H^{-1/2}(\Sigma) \times H^{1/2}(\Sigma)$  depends on the choice of the FEM-BEM coupling and involves Boundary Integral Operators (BIOs) (see Section 2). The linear form  $l_{\Omega_F}$  accounts for the contributions of the source term  $f$  and the boundary condition on  $\Omega_O$ . Here, the canonical duality pairing between a Banach space  $H$  and its topological dual  $H^*$  is denoted  $\langle \cdot, \cdot \rangle: H^* \times$

$H \rightarrow \mathbb{C}$  and defined by  $\langle \varphi, v \rangle := \varphi(v)$ . We emphasize that the duality pairings we consider do *not* involve any complex conjugation.

Next, we introduce a boundary operator  $B_\Sigma: H^{1/2}(\Sigma) \times H^{-1/2}(\Sigma) \rightarrow H^{1/2}(\Sigma)$ , defined by  $B_\Sigma(\phi, p) := \phi$ , and also consider a *transmission* (or *impedance*) operator  $T_\Sigma: H^{1/2}(\Sigma) \rightarrow H^{-1/2}(\Sigma)$ , satisfying  $\langle T_\Sigma(\phi), \bar{\phi} \rangle > 0 \quad \forall \phi \in H^{1/2}(\Sigma) \setminus \{0\}$ ,  $T_\Sigma^* = T_\Sigma$ , and  $\operatorname{Re}(T_\Sigma) > 0$ . The scattering operator  $S_B$  involved in the GOSM is given by  $\operatorname{Id} + 2\iota T_\Sigma B_\Sigma (A_\Sigma - \iota B_\Sigma^* T_\Sigma B_\Sigma)^{-1} B_\Sigma^*$ . We aim to study the kernel of  $A_\Sigma - \iota B_\Sigma^* T_\Sigma B_\Sigma$ , which is crucial to establishing the well-posedness of the GOSM.

## 2 Boundary integral operators and kernel of $A_\Sigma - \iota B_\Sigma^* T_\Sigma B_\Sigma$

The *Dirichlet-Neumann trace map* on  $\Sigma$  (from  $\Omega_B$ ),  $\gamma: H_{\text{loc}}^1(\Delta, \overline{\Omega_B}) \rightarrow H^{1/2}(\Sigma) \times H^{-1/2}(\Sigma)$ , is defined as the unique bounded linear operator satisfying  $\gamma(\varphi) := (\gamma_D(\varphi), \gamma_N(\varphi)) := (\varphi|_\Sigma, \mathbf{n}_B \cdot \nabla \varphi|_\Sigma), \forall \varphi \in \mathcal{C}^\infty(\overline{\Omega_B}) := \{\varphi|_\Omega, \varphi \in \mathcal{C}^\infty(\mathbb{R}^d)\}$ , where  $\mathbf{n}_B$  is the unit normal on  $\partial\Omega_B$  directed toward the exterior of  $\Omega_B$ .

Next, denote  $\mathcal{G}_\kappa$  the outgoing Helmholtz *Green kernel* with wavenumber  $\kappa > 0$ , satisfying  $(\Delta + \kappa^2)\mathcal{G}_\kappa = \delta$  in  $\mathbb{R}^d$  where  $\delta$  is the Dirac delta function. For  $d = 3$ ,  $\mathcal{G}_\kappa(\mathbf{x}) := \exp(\iota\kappa|\mathbf{x}|)/(4\pi|\mathbf{x}|)$ , and for  $d = 2$   $\mathcal{G}_\kappa(\mathbf{x}) := \iota H_0^{(1)}(\kappa|\mathbf{x}|)/(4\pi)$ , with  $H_0^{(1)}$  the 0-th order Hankel function of the first kind [7, Chapter 9]. For any  $\mathbf{x} \in \mathbb{R}^d \setminus \Sigma$ , and sufficiently smooth traces  $(v, p)$ , define the *total layer potential operator* by

$$G_\Sigma(v, p)(\mathbf{x}) := \int_\Sigma \mathbf{n}_B(\mathbf{y}) \cdot (\nabla \mathcal{G}_\kappa)(\mathbf{x} - \mathbf{y}) v(\mathbf{y}) + \mathcal{G}_\kappa(\mathbf{x} - \mathbf{y}) p(\mathbf{y}) \, ds(\mathbf{y}), \quad (4)$$

where  $ds$  refers to the Lebesgue surface measure on  $\Sigma$ . The map  $(v, p) \mapsto G_\Sigma(v, p)|_{\Omega_B}$  can be extended by density as a bounded linear operator  $H^{1/2}(\Sigma) \times H^{-1/2}(\Sigma) \rightarrow H_{\text{loc}}^1(\Delta, \Omega_B)$ . For any pair  $(v, p) \in H^{1/2}(\Sigma) \times H^{-1/2}(\Sigma)$ , the function  $u := G_\Sigma(v, p)$  solves the Helmholtz equation with wavenumber  $\kappa$  in  $\mathbb{R}^d \setminus \Sigma$ , see e.g. [10, §3.1], and satisfies Sommerfeld's radiation condition, see [8].

Using the Dirichlet-Neumann trace map  $\gamma$ , we form the *Calderón projector*  $\gamma \cdot G_\Sigma: H^{1/2}(\Sigma) \times H^{-1/2}(\Sigma) \rightarrow H^{1/2}(\Sigma) \times H^{-1/2}(\Sigma)$ , commonly decomposed as

$$\gamma \cdot G_\Sigma = \frac{1}{2} \begin{bmatrix} \operatorname{Id} & 0 \\ 0 & \operatorname{Id} \end{bmatrix} + \begin{bmatrix} K_\kappa & V_\kappa \\ W_\kappa & \tilde{K}_\kappa \end{bmatrix},$$

where the four classical *Boundary Integral Operators* (BIOs) appear:  $V_\kappa: H^{-1/2}(\Sigma) \rightarrow H^{1/2}(\Sigma)$  (*single layer*),  $K_\kappa: H^{1/2}(\Sigma) \rightarrow H^{1/2}(\Sigma)$  (*double layer*),  $\tilde{K}_\kappa: H^{-1/2}(\Sigma) \rightarrow H^{-1/2}(\Sigma)$  (*adjoint double layer*), and  $W_\kappa: H^{1/2}(\Sigma) \rightarrow H^{-1/2}(\Sigma)$  (*hypersingular*). Both  $V_\kappa$  and  $W_\kappa$  are symmetric, while  $K_\kappa^* = -\tilde{K}_\kappa$ . We recall that the adjoint  $*$  does not involve complex conjugation.

These BIOs naturally arise when deriving Boundary Integral Equations for Dirichlet or Neumann boundary conditions. For instance, for  $u \in H^1(\Omega_B)$  such that  $\Delta u + \kappa^2 u = 0$  in  $\Omega_B$ , they appear in the *Calderón equations* (see [10, Sect. 3.4])

$$(\text{Id}/2 - K_\kappa)\gamma_D(u) = V_\kappa \gamma_N(u), \quad (5a)$$

$$(\text{Id}/2 - \tilde{K}_\kappa)\gamma_N(u) = W_\kappa \gamma_D(u). \quad (5b)$$

Alternatively, combinations of these BIORs arise when dealing with an outgoing impedance boundary condition  $\mathbf{n}_B \cdot \nabla u|_\Sigma - i T_\Sigma u|_\Sigma = g, g \in H^{-1/2}(\Sigma)$ . For instance, subtracting  $i V_\kappa T_\Sigma \gamma_D(u)$  in Equation (5a) yields  $D_{\kappa, T_\Sigma}^* \gamma_D(u) = V_\kappa(g)$ , where we introduced the *impedance BIOR*  $D_{\kappa, T_\Sigma}^* := (\text{Id}/2 - K_\kappa) - i V_\kappa T_\Sigma$ . Other impedance BIORs could be derived using the Calderón equation (5b), but we do not focus on them.

For particular values of  $\kappa$ , called *spurious resonances*,  $V_\kappa, K_\kappa, \tilde{K}_\kappa$  and  $W_\kappa$  are well known to be singular [3, 7, 10]. A similar result holds for the impedance BIOR  $D_{\kappa, T_\Sigma}^*$ , see [3, Sect. 2.6].

**Lemma 1** *We have  $\ker(D_{\kappa, T_\Sigma}^*) \neq \{0\}$  if and only if the homogeneous Dirichlet Helmholtz problem set in  $\mathbb{R}^d \setminus \overline{\Omega}_B$  with wavenumber  $\kappa$  has a non-trivial solution. The elements of  $\ker(D_{\kappa, T_\Sigma}^*)$  are the Dirichlet traces of solutions to Helmholtz problems set in  $\Omega_B$  with non-homogeneous impedance boundary condition  $g \in \ker(V_\kappa)$ .*

*Remark 1* Since  $\Omega_B$  is a connected unbounded domain with bounded boundary,  $\ker(V_\kappa) = \ker(\text{Id}/2 + \tilde{K}_\kappa) = \ker(D_{\kappa, T_\Sigma})$ . When  $\Omega_B$  is bounded,  $\ker(V_\kappa) = \ker(\text{Id}/2 + \tilde{K}_\kappa) \neq \ker(D_{\kappa, T_\Sigma})$ .

Because of spurious resonances, classical FEM-BEM formulations can be non-uniquely solvable at certain wavenumbers, even when (1) is well-posed, see [11]. The classical Johnson-Nédélec and Costabel couplings are of the form (3) by taking respectively

$$A_{\Sigma, \text{JN}} := \begin{bmatrix} 0 & \text{Id} \\ \text{Id}/2 - K_\kappa & -V_\kappa \end{bmatrix} \quad \text{and} \quad A_{\Sigma, \text{C}} := \begin{bmatrix} W_\kappa & \text{Id}/2 + \tilde{K}_\kappa \\ \text{Id}/2 - K_\kappa & -V_\kappa \end{bmatrix}.$$

We now establish that the GOSM reformulations (2) of these FEM-BEM formulations suffer from the same spurious resonances. Indeed, the inverse of  $A_\Sigma - i B_\Sigma^* T_\Sigma B_\Sigma$  is needed to define  $S_B$ , but, due to spurious resonances,  $A_\Sigma - i B_\Sigma^* T_\Sigma B_\Sigma$  can be singular. In the following proofs, note that  $B_\Sigma^*(p) = (p, 0)$ , so  $B_\Sigma^* T_\Sigma B_\Sigma(\phi, p) = (T_\Sigma \phi, 0)$ .

**Proposition 1 (Johnson-Nédélec coupling)** *If  $A_\Sigma = A_{\Sigma, \text{JN}}$ , then*

$$\ker(A_\Sigma - i B_\Sigma^* T_\Sigma B_\Sigma) = \{(\phi, i T_\Sigma \phi) \mid \phi \in \ker(D_{\kappa, T_\Sigma}^*)\}.$$

*Proof.*  $(\phi, p) \in \ker(A_\Sigma - i B_\Sigma^* T_\Sigma B_\Sigma)$  if and only if  $[-i T_\Sigma \phi + p = 0 \text{ and } (\text{Id}/2 - K_\kappa)\phi - V_\kappa p = 0]$ , which is equivalent to  $[p = i T_\Sigma \phi \text{ and } D_{\kappa, T_\Sigma}^* \phi = 0]$ .  $\square$

**Proposition 2 (Costabel coupling)** *If  $A_\Sigma = A_{\Sigma, \text{C}}$ , then*

$$\ker(A_\Sigma - i B_\Sigma^* T_\Sigma B_\Sigma) = \{(0, p) \mid p \in \ker(D_{\kappa, T_\Sigma}^*)\}.$$

*Proof.* We first prove  $(\subset)$ . Let  $(\phi, p) \in \ker(A_\Sigma - i B_\Sigma^* T_\Sigma B_\Sigma)$ . Then

$$(W_\kappa - \iota T_\Sigma)\phi + (\text{Id}/2 + \tilde{K}_\kappa)p = 0, \quad (\text{Id}/2 - K_\kappa)\phi - V_\kappa p = 0. \quad (6)$$

Let  $w := G_\Sigma(\phi, p)$  and apply the Dirichlet-Neumann trace operator  $\gamma$  on  $w$  to obtain  $\gamma_D(w) = (\text{Id}/2 + K_\kappa)\phi + V_\kappa p$  and  $\gamma_N(w) = W_\kappa\phi + (\text{Id}/2 + \tilde{K}_\kappa)p$ . It follows from Equation (6) that  $\phi = \gamma_D(w)$  and  $\gamma_N(w) = \iota T_\Sigma\phi$ . The impedance trace  $\gamma_N(w) - \iota T_\Sigma\gamma_D(w)$  is then null. Since by construction  $w$  is solution to the Helmholtz equation in  $\Omega_B$  and satisfies Sommerfeld's radiation condition,  $w = 0$ , and so  $\phi = 0$ . Using  $T_\Sigma$  to combine the two equations of (6), we conclude that  $p \in \ker(D_{\kappa, T_\Sigma})$ .

To prove  $(\supset)$ , observe that according to Remark 1,  $p \in \ker(D_{\kappa, T_\Sigma}) = \ker(V_\kappa) = \ker(\text{Id}/2 + \tilde{K}_\kappa)$ , so we directly obtain the relations in Equation (6) for  $\phi = 0$ .  $\square$

*Remark 2* Propositions 1–2 still hold when  $A_\Sigma$  is derived from a bounded domain, even though Remark 1 no more holds. The proofs are even simpler since  $\ker(D_{\kappa, T_\Sigma}^*)$  and  $\ker(D_{\kappa, T_\Sigma})$  are both reduced to the trivial element, so is  $\ker(A_\Sigma - \iota B_\Sigma^* T_\Sigma B_\Sigma)$ .

*Remark 3* Most of the restrictions imposed on the geometry in Section 1 have been made to simplify the expression of the variational formulation (3), and those of the kernels in Propositions 1–2. The expressions of the kernels hold when  $\Omega_B$  is still connected, but  $\Omega_F$  is not connected or  $\partial\Omega_O \not\subseteq \partial\Omega_F$  (see e.g. Figure 1 (right)), by taking care of considering  $\partial\Omega_B$  instead of  $\Sigma$ .

### 3 Numerical illustration

We consider the scattering of an incoming plane wave  $u_i(r, \theta) = \exp(\iota\kappa r \cos \theta)$ , where  $(r, \theta)$  are the polar coordinates, by a sound-soft obstacle  $\mathcal{D} = \Omega_O$ , which is a disk of radius 1. The whole domain  $\Omega = \mathbb{R}^d \setminus \mathcal{D}$  is assumed homogeneous, that is,  $\kappa = k > 0$  constant. This can be modeled by Problem (1) with (non-homogeneous) Dirichlet boundary conditions and  $f = 0$ , whose unique solution is

$$u_S(r, \theta) := - \sum_{p \in \mathbb{Z}} \exp(\iota p \theta) \iota^{|p|} J_{|p|}(\kappa r) \frac{H_{|p|}^1(\kappa r)}{H_{|p|}^1(\kappa)},$$

with  $J_\nu$  and  $H_\nu^1$  respectively the Bessel and Hankel function of first kind of order  $\nu$ . Here,  $\Omega_F$  is the annulus of radii 1 and 2, and  $\Omega_B = \Omega \setminus (\overline{\Omega_F} \cup \overline{\Omega_O})$ , see Figure 1(left).

As transmission operator  $T_\Sigma$  in the BEM domain we choose  $W_{i\kappa}$ , the hypersingular operator for the *Yukawa operator*, that is,  $-\Delta + \kappa^2 \text{Id}$ . As transmission operator  $T_{\Omega_F}$  in the FEM domain we choose a Schur complement-based operator relying on the discretization of a positive Dirichlet-to-Neumann map for the Yukawa operator, see [9, Chapter 8]. For more details about the expression of the chosen transmission operators, we refer to [2, Sect. 10.2]. We use  $\mathbb{P}_1$ -Lagrange finite and boundary elements. Finite element (resp. boundary element) matrices are stored in sparse (resp. dense) format. For the sake of simplicity, for the discrete unknowns, we use

the same notations as for the continuous unknowns. The numerical solution of the GOSM substructured formulation (2) is obtained using the GMRes method.

The spurious resonances for the considered geometry are the zeros of the first kind Bessel functions. We assume that  $\kappa$  is not a spurious resonance, so  $A_\Sigma - i B_\Sigma^* T_\Sigma B_\Sigma$  is invertible. To illustrate the sensitivity or the robustness to spurious resonances of the GOSM for the Johnson-Nédélec and Costabel couplings, we study how the relative error of several quantities of interest evolves with respect to  $\kappa$ . We focus on the wavenumber range  $\kappa \in [4.28, 4.42]$ , inside which only  $\kappa_1 \approx 4.32685$  and  $\kappa_2 \approx 4.38575$  are spurious resonances. All the experiments have been led with a fixed mesh generated for  $\kappa = 10$  and 20 points per wavelength.

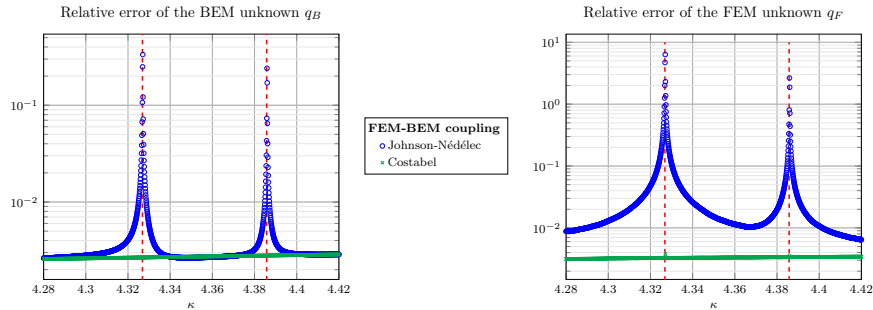


Fig. 2: Relative error of the BEM (left) and FEM (right) unknowns.

Our first quantity of interest is the BEM unknown  $q_B$ . In Figure 2 (left) we observe, for the Johnson-Nédélec coupling, peaks in the relative error of  $q_B$  when  $\kappa$  is close to the spurious resonances  $\kappa_1$  and  $\kappa_2$ . No peaks are observed in the curve associated with the Costabel coupling. These results may be interpreted given the explicit expressions of the coupling kernels stated in Propositions 1–2, and of the scattering operator  $S_B$  (see the end of Section 1). First, assume we want to compute  $S_B q$  for a given vector  $q$ , and denote  $v_q := (A_\Sigma - i B_\Sigma^* T_\Sigma B_\Sigma)^{-1} B_\Sigma^* q$ . Because of the definition of  $B_\Sigma$  only the first component of  $v_q$  is relevant to compute  $S_B q = q + 2i T_\Sigma B_\Sigma v_q$ . Second, when  $\kappa$  is a spurious resonance only the second component of the eigenvectors of the Costabel operator  $A_\Sigma - i B_\Sigma^* T_\Sigma B_\Sigma$  is non-trivial. Thus, when numerically inverting that operator near a spurious resonance, we can expect the first component of  $v_q$  to be of good accuracy, while the second might be less accurate. Turning to the eigenvectors of the Johnson-Nédélec operator, both components are non-trivial, so both components of  $v_q$  might deteriorate (especially the first one).

Next, we study the relative error of the FEM unknown  $q_F$ , shown in Figure 2 (right). As for the BEM curve, we observe peaks around spurious resonances only when considering the Johnson-Nédélec coupling. Nonetheless, we emphasize that  $A_{\Omega_F} - i B_{\Omega_F}^* T_{\Omega_F} B_{\Omega_F}$  is invertible, whatever the wavenumber. The reasoning used to explain the growth of the relative error of the BEM unknown  $q_B$  can not hold for  $q_F$ . This suggests that, near a spurious resonance, the poor quality of  $q_B$  makes also

$q_F$  less accurate. Remembering that  $q_F$  and  $q_B$  are the data shared between the FEM and BEM subdomains, that observation is not surprising.

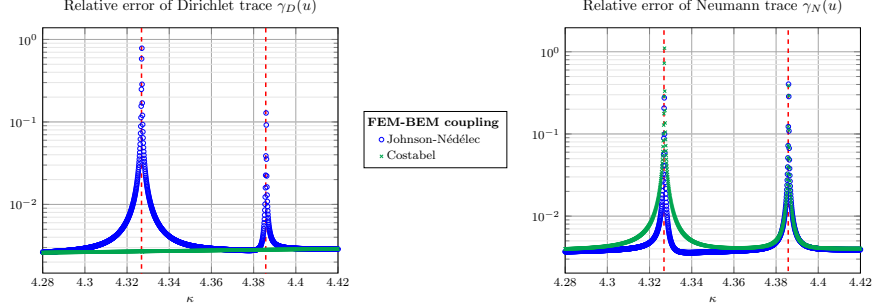


Fig. 3: Relative errors of reconstructed Dirichlet (left) and Neumann (right) traces.

We now turn to the evolution of the relative errors of  $\gamma_D(u)$  and  $\gamma_N(u)$ , with respect to  $\kappa$ . We emphasize that  $\gamma_D(u)$  and  $\gamma_N(u)$  are *reconstructed* from the solution of the GOSM, namely  $(\gamma_D(u), \gamma_N(u)) := (A_\Sigma - i B_\Sigma^* T_\Sigma B_\Sigma)^{-1} B_\Sigma^* q_B = v_{q_B}$ . In Figure 3, when  $\kappa$  is close to a spurious resonance we observe peaks only in the Neumann relative error curve for the Costabel coupling, while there are peaks in both Dirichlet and Neumann curves for the Johnson-Nédélec coupling. The results confirm what we said previously about the deterioration near a spurious resonance of the components of  $v_q$  for a given vector  $q$ . It is interesting to note that the reconstructed solution  $(\gamma_D(u), \gamma_N(u))$  is more and more polluted when  $\kappa$  becomes closer to a spurious resonance, even though  $A_\Sigma - i B_\Sigma^* T_\Sigma B_\Sigma$  is invertible. We highlight that the relative errors go from 1% to more than 100%, but are not comparable: around  $\kappa_1$  the Dirichlet relative error is close to 1, while the Neumann relative error is close to 0.4. These two errors are too large for  $q_B$  and the reconstructed solution to be considered as good quality approximations.

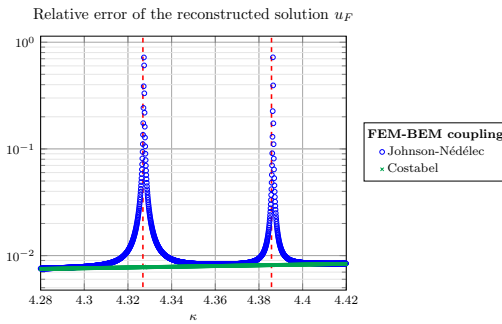


Fig. 4: Relative error of the reconstructed solution  $u_F$  in the FEM domain.

We end by looking at Figure 4, which shows the relative error of  $u_F$ , the reconstructed volume solution in  $\Omega_F$ , with respect to  $\kappa$ . We observe peaks around spurious resonances for the Johnson-Nédélec coupling, which are consequences of the peaks observed for  $q_F$  in Figure 2 (right). Moreover, it is coherent to recover an error for the solution in  $\Omega_F$  for the Johnson-Nédélec coupling, because its Dirichlet trace should be equal to  $\gamma_D(u)$ , for which we have also observed a peak in the relative error. On the other hand, for the same reason, it is coherent to not observe any peak in the relative error when the Costabel coupling is used.

Finally, we pinpoint that relative errors peaks arise in the same way when classical FEM-BEM couplings (3) are considered. Indeed, for a geometry with two subdomains without an obstacle, it has been proven that only the Neumann component of the Costabel coupling can be polluted, see for instance [11, Theorem 1], while for the Johnson-Nédélec coupling both volume and Neumann components can be polluted.

## References

1. Bielak, J., MacCamy, R.C.: An exterior interface problem in two-dimensional elastodynamics. *Quarterly of Applied Mathematics* **41**(1), 143–159 (1983). DOI 10.1090/qam/700668
2. Boisneault, A., Bonazzoli, M., Claeys, X., Marchand, P.: Discrete FEM-BEM coupling with a Generalized Optimized Schwarz Method. In preparation
3. Chandler-Wilde, S., Graham, I., Langdon, S., Spence, E.: Numerical-asymptotic boundary integral methods in high-frequency acoustic scattering. *Acta Numerica* **21**, 89–305 (2012). DOI 10.1017/s0962492912000037
4. Claeys, X.: Nonlocal optimized Schwarz method for the Helmholtz equation with physical boundaries. *SIAM J. Math. Anal.* **55**(6), 7490–7512 (2023). DOI 10.1137/23M1545847
5. Costabel, M.: Symmetric methods for the coupling of finite elements and boundary elements. In: *Mathematical and Computational Aspects*, pp. 411–420. Springer Berlin Heidelberg (1987). DOI 10.1007/978-3-662-21908-9\_26
6. Johnson, C., Nédélec, J.C.: On the coupling of boundary integral and finite element methods. *Math. of Comput.* **35**(152), 1063–1079 (1980). DOI 10.1090/s0025-5718-1980-0583487-9
7. McLean, W.C.H.: *Strongly elliptic systems and boundary integral equations*. Cambridge University Press (2000)
8. Nédélec, J.C.: Acoustic and electromagnetic equations, *Applied Mathematical Sciences*, vol. 144. Springer-Verlag, New York (2001). DOI 10.1007/978-1-4757-4393-7. Integral representations for harmonic problems
9. Parolin, E.: Non-overlapping domain decomposition methods with non-local transmission operators for harmonic wave propagation problems. Phd thesis, IP Paris (2020). URL <https://theses.hal.science/tel-03118712>
10. Sauter, S.A., Schwab, C.: *Boundary element methods*, *Springer Series in Computational Mathematics*, vol. 39. Springer-Verlag, Berlin (2011). DOI 10.1007/978-3-540-68093-2
11. Schulz, E., Hiptmair, R.: Spurious resonances in coupled domain-boundary variational formulations of transmission problems in electromagnetism and acoustics. *Computational Methods in Applied Mathematics* **22**(4), 971–985 (2022). DOI 10.1515/cmam-2021-0197